

Photoluminescence study of lateral confinement energy in T-shaped $\text{In}_x\text{Ga}_{1-x}\text{As}$ quantum wires

Hidefumi Akiyama

Institute for Solid State Physics (ISSP), University of Tokyo, and Quantum Transition Project, Japan Science and Technology Corporation, 7-22-1 Roppongi, Minato-ku, Tokyo 106, Japan

Takao Someya

Institute of Industrial Science (IIS), and Research Center for Advanced Science and Technology (RCAST), University of Tokyo, 7-22-1 Roppongi, Minato-ku, Tokyo 106, Japan

Masahiro Yoshita and Takeaki Sasaki

Institute for Solid State Physics (ISSP), University of Tokyo, 7-22-1 Roppongi, Minato-ku, Tokyo 106, Japan

Hiroyuki Sakaki

Quantum Transition Project, Japan Science and Technology Corporation, and Institute of Industrial Science (IIS), and Research Center for Advanced Science and Technology (RCAST), University of Tokyo, 4-7-6 Komaba, Meguro-ku, Tokyo 153, Japan

(Received 16 September 1997)

A study of high-quality $\text{In}_x\text{Ga}_{1-x}\text{As}$ T-shaped quantum wires (T-QWR's) via photoluminescence spectroscopy to characterize the lateral confinement effect is reported. The effective lateral confinement energy of excitons in 3.5-nm-scale $\text{In}_{0.17}\text{Ga}_{0.83}\text{As}/\text{Al}_{0.3}\text{Ga}_{0.7}\text{As}$ T-QWR's is found to be as large as 34 meV. The value has been examined in comparison with the previous results on $\text{GaAs}/\text{Al}_{0.3}\text{Ga}_{0.7}\text{As}$ and GaAs/AlAs T-QWR's. [S0163-1829(98)00304-X]

To study one-dimensional (1D) optical properties of quantum wires (QWR's),^{1,2} T-shaped QWR's (T-QWR's) have been developed via the cleaved edge overgrowth (CEO) method with molecular-beam epitaxy (MBE),^{3,4} in which the 1D electronic state is formed at the T intersection of two parent quantum wells (QW's), namely, the first-growth QW (QW1, thickness a) for the "stem" part of letter "T," and the second-growth QW (QW2, thickness b) for the "arm" part of it.

Early successful growth of a series of samples was realized in GaAs T-QWR's with $\text{Al}_{0.3}\text{Ga}_{0.7}\text{As}$ barrier (shortly denoted as $\text{GaAs}/\text{Al}_{0.3}\text{Ga}_{0.7}\text{As}$ T-QWR's), which were used in some systematic experiments for the physics of 1D excitons.⁵⁻⁹ However, the effective lateral confinement energy of excitons $E_{1\text{D}-2\text{D}}^*$, which represents the stability of 1D excitons and is defined as the energy separation between 1D and 2D excitons, is only 18 meV in the 5-nm-scale $\text{GaAs}/\text{Al}_{0.3}\text{Ga}_{0.7}\text{As}$ T-QWR's.⁹

It is to be noted that strong lateral confinement is important to realize remarkable 1D properties. The straightforward way to enhance the effective lateral confinement energy $E_{1\text{D}-2\text{D}}^*$ in T-QWR's is to enhance the quantization energy E_Q of the parent QW's. (In the infinite barrier approximation, these two quantities should be proportional.) For this purpose, we need to increase barrier energy or to decrease well energy, rather than merely to reduce QW thickness. Previously, we increased barrier energy by replacing the $\text{Al}_{0.3}\text{Ga}_{0.7}\text{As}$ barrier with the AlAs barrier, and realized $E_{1\text{D}-2\text{D}}^* = 38$ meV.⁹⁻¹¹

Now we investigate the effect of decreasing the well energy by introducing $\text{In}_x\text{Ga}_{1-x}\text{As}$. The points are, first, to overcome the difficult growth of $\text{In}_x\text{Ga}_{1-x}\text{As}$ on the (110)

surface and fabricate high-quality $\text{In}_x\text{Ga}_{1-x}\text{As}/\text{Al}_{0.3}\text{Ga}_{0.7}\text{As}$ T-QWR's, and, second, to establish a quantitative understanding of the lateral confinement energy in T-QWR's made of our material system.

In this paper we report a study of high-quality $\text{In}_x\text{Ga}_{1-x}\text{As}/\text{Al}_{0.3}\text{Ga}_{0.7}\text{As}$ T-QWR's and their lateral confinement energy, in comparison with the previous results on $\text{GaAs}/\text{Al}_{0.3}\text{Ga}_{0.7}\text{As}$ and GaAs/AlAs T-QWR's. Three 4-nm-scale $\text{In}_{0.09}\text{Ga}_{0.91}\text{As}/\text{Al}_{0.3}\text{Ga}_{0.7}\text{As}$ T-QWR samples (samples $N1-N3$) and one 3.5-nm-scale $\text{In}_{0.17}\text{Ga}_{0.83}\text{As}/\text{Al}_{0.3}\text{Ga}_{0.7}\text{As}$ T-QWR sample (sample $N4$) have been studied, which are schematically shown in the inset of Figs. 1 and 2.

The fabrication procedure¹² of samples $N1-N3$ was as follows. On a semi-insulating (001) GaAs substrate, we successively grew a 500-nm GaAs buffer layer, a 5- μm $\text{Al}_{0.3}\text{Ga}_{0.7}\text{As}$ layer, ten periods of 4-nm-thick $\text{In}_{0.09}\text{Ga}_{0.91}\text{As}$ multiple QW's and 100-nm-thick $\text{Al}_{0.3}\text{Ga}_{0.7}\text{As}$ barriers for QW1, a 10-nm AlAs layer, a 5- μm $\text{Al}_{0.3}\text{Ga}_{0.7}\text{As}$ layer, a 10-nm AlAs layer, and a 500-nm GaAs cap layer, by the conventional MBE method under a constant substrate temperature T_s of 560 °C, a V/III flux ratio of ~ 2 , and a GaAs growth rate of 0.7 $\mu\text{m}/\text{h}$. On the *in situ* cleaved (110) surface of this wafer which was prepared by the method described in Ref. 12, we then grew at $T_s = 430$ °C an $\text{In}_{0.09}\text{Ga}_{0.91}\text{As}$ layer of thickness b for QW2, and a 2-ML-thick $\text{Al}_{0.3}\text{Ga}_{0.7}\text{As}$ cover layer; then, at $T_s = 500$ °C, a 10-nm-thick $\text{Al}_{0.3}\text{Ga}_{0.7}\text{As}$ barrier layer and a 10-nm-thick GaAs cap layer. The V/III flux ratio was 30, and the $\text{In}_{0.09}\text{Ga}_{0.91}\text{As}$ growth rate was 0.5 $\mu\text{m}/\text{h}$. The growth condition of $\text{In}_x\text{Ga}_{1-x}\text{As}$ on the (110) surface was optimized by the repeated test growth and characterization, which was essential for the fabrication of the $\text{In}_x\text{Ga}_{1-x}\text{As}$ T-QWR's.¹³ Three samples were formed by the same first growth and the three different CEO runs, changing the parameter b around 4 nm.

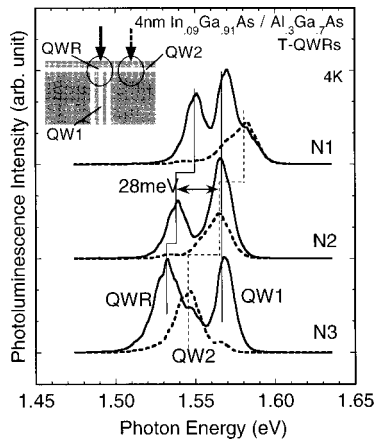


FIG. 1. The spatially resolved PL spectra of three 4-nm-scale $\text{In}_{0.09}\text{Ga}_{0.91}\text{As}/\text{Al}_{0.3}\text{Ga}_{0.7}\text{As}$ T-QWR samples with identical QW1 thickness a and different QW2 thicknesses b (samples $N1-N3$ shown schematically in the inset) measured from above the (110) CEO surface at 4 K with 633-nm excitation light from a He-Ne laser. Solid curves show the PL spectra for the 1- μm -wide region on QW1 and QWR's, while the dashed curves show those for the 5- μm -wide regions of QW2.

The above structure parameters used in the MBE growth are nominal. We calibrated the values of a and b in the photoluminescence (PL) experiment shown below, which are $a=4.1$ nm and $b=3.5$ (sample $N1$), 3.9 (sample $N2$), and 4.4 (sample $N3$) nm.

To realize stronger confinement, we also prepared a 3.5-nm-scale $\text{In}_{0.17}\text{Ga}_{0.83}\text{As}/\text{Al}_{0.3}\text{Ga}_{0.7}\text{As}$ T-QWR sample as sample $N4$. Its fabrication procedure was the same as that of samples $N1-N3$, except for the increased In content of 17% and the reduced QW thickness of 3.5 nm. The calibrated values of a and b are $a=3.7$ nm and $b=3.4$ nm.

Note that base structures formed by the first growth of all the samples are totally 1- μm -thick layers of QW1 and 5- μm -thick $\text{Al}_{0.3}\text{Ga}_{0.7}\text{As}$ layers on both sides, so that CEO makes a 1- μm -wide region with QWR's sandwiched by 5- μm -wide QW2 regions, as schematically shown in the insets

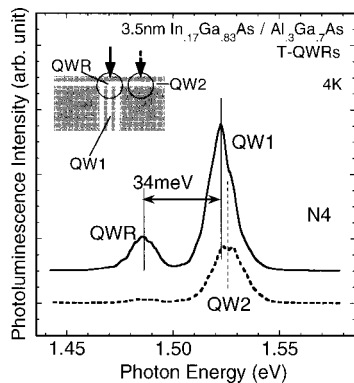


FIG. 2. The spatially resolved PL spectra of the 3.5-nm-scale $\text{In}_{0.17}\text{Ga}_{0.83}\text{As}/\text{Al}_{0.3}\text{Ga}_{0.7}\text{As}$ T-QWR sample (sample $N4$ shown schematically in the inset) measured from above the (110) CEO surface at 4 K with 633-nm excitation light from a He-Ne laser. The solid curve shows the PL spectra for the 1- μm -wide region on QW1 and QWR's, while the dashed curve shows those for the 5- μm -wide regions of QW2.

of Figs. 1 and 2. Thus spatially resolved PL spectroscopy^{11,12} was possible for these respective regions from above the (110) CEO surface at 4 K, with 633-nm excitation light from a He-Ne laser.

Figure 1 shows the spatially resolved PL spectra of the samples $N1-N3$. Solid curves show the PL spectra for the 1- μm -wide region on QW1 and QWR's, while the dashed curves show those for the 5- μm -wide regions of QW2. The origins of the three PL peaks in each sample were assigned to QW1, QW2, and QWR, as shown in the figure. The PL peaks of QW1 in the three samples stay at the same energy, because the thickness a is constant. On the other hand, as the thickness b is increased, the PL peaks of QW2 shift to the low-energy side as well as those of QWR's. The spectral linewidths of the three PL peaks were 15, 20, and 15 meV for QW1, QW2, and QWR in sample $N2$, respectively. The precise energy of each structure was determined by these spectra.

The effective lateral confinement energy of excitons $E_{1\text{D-2D}}^*$ in T-QWR's is defined as the energy difference between the QWR and the lower-energy QW between QW1 and QW2, which represents the stabilization energy of 1D excitons. From the observed peak energies, $E_{1\text{D-2D}}^*$ of samples $N1, N2$, and $N3$ were determined as 19, 28, and 15 meV, respectively. It reached a maximum of 28 meV in sample $N2$, where the PL energies of QW1 and QW2 are equal.

Figure 2 shows the spatially-resolved PL spectra of the 3.5-nm-scale $\text{In}_{0.17}\text{Ga}_{0.83}\text{As}/\text{Al}_{0.3}\text{Ga}_{0.7}\text{As}$ T-QWR samples (samples $N4$). Solid and dashed curves show the PL spectra for the 1- μm -wide region on QW1 and QWR's, and the 5- μm -wide regions of QW2, respectively. Similarly to samples $N1-N3$, three PL peaks assigned to QW1, QW2, and QWR's have been observed. The spectral linewidths of three PL peaks were 13, 17, and 14 meV for QW1, QW2, and the QWR, respectively. The increased effective lateral confinement energy was realized in sample $N4$, that was $E_{1\text{D-2D}}^* = 34$ meV.

These series of well-resolved PL spectra demonstrate that the designed high-quality $\text{In}_x\text{Ga}_{1-x}\text{As}$ T-QWR's are available, as well as the previous GaAs T-QWR's. A detailed microscopic characterization of these $\text{In}_x\text{Ga}_{1-x}\text{As}$ T-QWR's, to ensure the assignment, and more importantly to demonstrate the high uniformity of the samples, will be reported elsewhere.¹⁴

To investigate the lateral confinement of each sample, we performed supplementary PL measurements for bulklike reference samples. From reference samples for $N1-N3$, the band-gap energies E_g at 4 K with no confinement were obtained for $\text{In}_{0.09}\text{Ga}_{0.91}\text{As}$ on GaAs and $\text{Al}_{0.3}\text{Ga}_{0.7}\text{As}$, which are 1.421 and 1.885 eV, respectively. Since the PL energy of QW1 in samples $N1-N3$ is 1.567 eV, the quantization energy E_Q and the band-gap discontinuity ΔE_g for QW1 are derived to be 146 and 464 meV, respectively. As for sample $N4$, E_g of $\text{In}_{0.17}\text{Ga}_{0.83}\text{As}$ on GaAs and $\text{Al}_{0.3}\text{Ga}_{0.7}\text{As}$ are measured to be 1.344 and 1.901 eV, respectively. From the PL energy 1.520 eV of QW1, E_Q and ΔE_g for QW1 are 176 and 557 meV, respectively.

These results are summarized in Table I, together with the values for the 5-nm-scale GaAs/ $\text{Al}_{0.3}\text{Ga}_{0.7}\text{As}$ (sample $S1$ in

TABLE I. Summary of the experimental results for four kinds of T-QWR samples: the effective lateral confinement energy of excitons E_{1D-2D}^* , which is maximized when QW1 and QW2 have the same PL energy, the quantization energy E_Q is the PL energy measured from the bulk band-gap energy in the QW's, and the band-gap discontinuity ΔE_g .

	Unit	<i>N4</i>	<i>N2</i>	<i>S1</i> (Ref. 9)	<i>S2</i> (Ref. 9)
<i>a</i> (nominal)	nm	3.5	4	5	5
In content in well	%	17	9	0	0
Al content in barrier	%	30	30	30	100
E_{1D-2D}^* (max.)	meV	34	28	18	38
E_Q	meV	176	146	94	148
ΔE_g	meV	557	464	374	1590
ratio E_{1D-2D}^*/E_Q	%	19	19	19	26

Ref. 9) and 5-nm-scale GaAs/AlAs T-QWR's (sample *S2* in Ref. 9). The listed values of E_{1D-2D}^* (max.) are for T-QWR's where the energies of QW1 and QW2 are equal, and E_{1D-2D}^* is maximized.

We should first point out, by comparing E_{1D-2D}^* in samples *N4*, *N2*, and *S1*, that E_{1D-2D}^* is increased from 18 to 34 meV by increasing the In content *x* and reducing the QW thickness in $\text{In}_x\text{Ga}_{1-x}\text{As}/\text{Al}_{0.3}\text{Ga}_{0.7}\text{As}$ T-QWR's. However, we could not go over $E_{1D-2D}^* = 38$ meV achieved in sample *S2*, or 5-nm-scale GaAs/AlAs T-QWR's, with these samples.

It is interesting to see the ratio E_{1D-2D}^*/E_Q shown in the table. The ratio for two $\text{In}_x\text{Ga}_{1-x}\text{As}/\text{Al}_{0.3}\text{Ga}_{0.7}\text{As}$ T-QWR's (samples *N4* and *N2*) is about 19%, close to that for the GaAs/Al_{0.3}Ga_{0.7}As T-QWR (sample *S1*), while that for the GaAs/AlAs T-QWR (sample *S2*) is as large as 26%.

In the infinite barrier and constant isotropic effective-mass approximation, E_{1D-2D}^*/E_Q in balanced ($a=b$) T-QWR's should be constant (17% for a tentatively assumed electron mass of $0.067m_0$ and a hole mass of $0.4m_0$) without excitonic effect, since all the single-particle energy levels are proportional to the inverse square of the wave-function size. With the enhanced excitonic effect in tightly confined T-QWR's, an increased ratio of E_{1D-2D}^*/E_Q should be observed.

This argument approximately holds in samples *S1* and *S2*. In fact, detailed analysis has shown that the slightly and significantly enhanced E_{1D-2D}^* in samples *S1* and *S2*, respectively, are caused by the slight and significant enhancement of the exciton binding energy.⁹

However, the finite barrier effect should be more important in samples *N4* and *N2*, since E_Q is already 30% of ΔE_g . We believe that this is the reason for the smaller values of E_{1D-2D}^*/E_Q in samples *N4* and *N2* than in sample *S2*. When narrow T-QWR's are formed with a finite barrier, the wave function tends to penetrate into the barrier. Thus the excitonic effect is not so enhanced as in higher barrier cases. Furthermore, even without the excitonic effect, the model calculation shows that E_{1D-2D}^* becomes more saturated for increased E_Q in lower barrier cases.^{9,15}

To investigate more quantitatively and gain physical insight into the data, we assumed the following parameters,¹⁶⁻¹⁹ and calculated the energy levels based on the simple effective mass approximation: the electron effective mass of $0.0647m_0$ ($0.0626m_0$), the hole effective mass

of $0.367m_0$ ($0.358m_0$) along [001], and $0.682m_0$ ($0.656m_0$) along [110] in $\text{In}_{0.09}\text{Ga}_{0.91}\text{As}$ ($\text{In}_{0.17}\text{Ga}_{0.83}\text{As}$) QW's. The conduction-band offset ratio was assumed to be 0.65. Though different choice of the band parameters gives slightly different estimation of the values, the discussed physics is almost unaffected.

With these assumptions, we are able to calibrate the thicknesses *a* and *b* with the observed PL peak energies, which turn out to be $a=4.1$ nm (samples *N1*–*N3*) $b=3.5$ nm (sample *N1*), 3.9 nm (sample *N2*), 4.4 nm (sample *N3*), $a=3.7$ nm (sample *N4*), and $b=3.4$ nm (sample *N4*), reasonably close to the nominal values.

Then we interpreted the PL spectral linewidths observed in Figs. 1 and 2. The energy difference caused by monolayer fluctuation of the QW thickness is about 15 meV/ML (1 ML=0.283 nm) and 11 meV/ML for QW's in samples *N4* and *N2*, respectively. Therefore, we estimate that the thickness fluctuation of QW1 is about 1 ML, whereas that of QW2 is 1–2 ML in these samples, showing the reasonably good MBE growth on the (110) surface.

Next we calculated the electron wave-function width σ_z in QW1 as the root-mean-square expectation value of the electron position. The values of σ_z in samples *N4*, *N2*, *S1*, and *S2* are 5.2, 5.6, 6.3, and 4.3 nm, respectively. In spite of the fact that the actual widths *a* and *b* of samples *N4* and *N2* are smaller (3.5–4 nm) than those of sample *S2* (~ 5 nm), the wave-function width σ_z is much larger, showing the finite barrier effect discussed above. It is considered reasonable that the largest E_{1D-2D}^* is realized in sample *S2*, in which the wave-function size is smallest.

So far, we have not mentioned the effect of strain.²⁰ Since the lattice constant of $\text{In}_x\text{Ga}_{1-x}\text{As}$ is larger than that of GaAs, the overgrown region on $\text{In}_x\text{Ga}_{1-x}\text{As}$ by CEO should have expanding strain compared with the overgrown region on GaAs and $\text{Al}_y\text{Ga}_{1-y}\text{As}$. In other words, the lattice in the T-QWR region should be expanded and have a decreased band-gap energy compared with QW1 and QW2 regions, which should contribute to enlarging E_{1D-2D}^* .

The question has been the magnitude of this contribution. There was a discussion whether the conduction-edge modulation in QW2 grown 25 nm above the cleaved edge of 7.1-nm-thick $\text{In}_{0.063}\text{Ga}_{0.937}\text{As}/\text{GaAs}$ QW1 is 30–40 meV or at least two orders of magnitude less.²⁰

It turns out, in our result on sample *N2*, where QW2 is grown just on the cleaved edge of 4.1-nm-thick $\text{In}_{0.09}\text{Ga}_{0.91}\text{As}/\text{Al}_{0.3}\text{Ga}_{0.7}\text{As}$ QW1, that the magnitude of such contribution is far less than 10 meV. This is because $E_{1\text{D-2D}}^* = 28$ meV in sample *N2* is increased from $E_{1\text{D-2D}}^* = 18$ meV in sample *S1* by only 10 meV, while the enhancement of $E_{1\text{D-2D}}^*$ expected proportionally to the increased $E_Q = 146$ meV in sample *N2* from $E_Q = 94$ meV in sample *S1* is also about 10 meV. Note that the ratio $E_{1\text{D-2D}}^*/E_Q$ is almost unchanged between samples *N2* and *S1*. Therefore, $E_{1\text{D-2D}}^*$, increased by 10 meV, is dominantly caused by the increased E_Q , that is, the tightening of confinement. Since the contribution of strain in sample *N2* is included in the 10 meV as the residual minor part, it is considered to be not more than a few meV. Further measurements and analysis should be necessary to resolve all possible contribution in $E_{1\text{D-2D}}^*$.²¹⁻²⁴

We should finally remark the point that large $E_{1\text{D-2D}}^* = 34$ meV is achieved without introducing AlAs barriers in 3.5-nm-scale $\text{In}_{0.17}\text{Ga}_{0.83}\text{As}/\text{Al}_{0.3}\text{Ga}_{0.7}\text{As}$ T-QWR's, though it is slightly smaller than $E_{1\text{D-2D}}^* = 38$ meV in previously reported 5-nm-scale GaAs/AlAs T-QWR's. This point is important, since the AlAs barrier has some drawbacks, espe-

cially in fabricating QWR lasers.^{5,25,26} First, a separately confined heterostructure is not possible, if an AlAs barrier is used to confine electrons. Second, *in situ* cleavage and layer-by-layer growth are more difficult with AlAs, and AlAs is rather easily oxidized and degraded, compared with $\text{Al}_{0.3}\text{Ga}_{0.7}\text{As}$. Third, to further increase $E_{1\text{D-2D}}^*$, we have more design flexibility left with $\text{In}_x\text{Ga}_{1-x}\text{As}$, whereas further reduction of QW thickness in a GaAs/AlAs QW results in a type-II structure, in which electrons are stabilized in the X valley of AlAs.

In conclusion, a series of high-quality $\text{In}_x\text{Ga}_{1-x}\text{As}/\text{Al}_{0.3}\text{Ga}_{0.7}\text{As}$ T-QWR's have been fabricated for the study of the effective lateral confinement energy $E_{1\text{D-2D}}^*$. In 3.5-nm-scale $\text{In}_{0.17}\text{Ga}_{0.83}\text{As}/\text{Al}_{0.3}\text{Ga}_{0.7}\text{As}$ T-QWR's, $E_{1\text{D-2D}}^*$ is measured to be as large as 34 meV, where the wave-function penetration into the barrier region is significant compared with the previously studied 5-nm-scale GaAs/AlAs and GaAs/AlAs T-QWR's. Further enhancement of $E_{1\text{D-2D}}^*$ is possible by increasing the In or Al content in the present T-QWR's.

This work was partly supported by a Grant-in-Aid from the Ministry of Education, Science, Sports, and Culture, Japan.

-
- ¹H. Sakaki, Jpn. J. Appl. Phys. **19**, L735 (1980).
²Y. Arakawa and H. Sakaki, Appl. Phys. Lett. **40**, 939 (1982).
³L. N. Pfeiffer, K. W. West, H. L. Störmer, J. P. Eisenstein, K. W. Baldwin, D. Gershoni, and J. Spector, Appl. Phys. Lett. **56**, 1697 (1990).
⁴A. R. Goñi, L. N. Pfeiffer, K. W. West, A. Pinczuk, H. U. Baranger, and H. L. Störmer, Appl. Phys. Lett. **61**, 1956 (1992).
⁵W. Wegscheider, L. N. Pfeiffer, M. M. Dignam, A. Pinczuk, K. W. West, S. L. McCall, and R. Hull, Phys. Rev. Lett. **71**, 4071 (1993).
⁶T. Someya, H. Akiyama, and H. Sakaki, Phys. Rev. Lett. **74**, 3664 (1995).
⁷H. Akiyama, T. Someya, and H. Sakaki, Phys. Rev. B **53**, R10 520 (1996).
⁸H. Akiyama, T. Someya, and H. Sakaki, Phys. Rev. B **53**, R16 160 (1996).
⁹T. Someya, H. Akiyama, and H. Sakaki, Phys. Rev. Lett. **76**, 2965 (1996).
¹⁰T. Someya, H. Akiyama, and H. Sakaki, Appl. Phys. Lett. **66**, 3672 (1995).
¹¹H. Akiyama, T. Someya, and H. Sakaki, Phys. Rev. B **53**, R4229 (1996).
¹²T. Someya, H. Akiyama, and H. Sakaki, J. Appl. Phys. **79**, 2522 (1996).
¹³T. Someya, H. Akiyama, and H. Sakaki, Jpn. J. Appl. Phys. **35**, 2544 (1996).
¹⁴M. Yoshita, H. Akiyama, T. Someya, and H. Sakaki, J. Appl. Phys. (to be published).
¹⁵L. N. Pfeiffer, H. Baranger, D. Gershoni, K. Smith, and W. Wegscheider, in *Low Dimensional Structures Prepared by Epitaxial Growth or Regrowth on Patterned Substrates*, Vol. 298 of *NATO Advanced Study Institute, Series E: Applied Sciences*, edited by K. Ebel *et al.* (Kluwer, Dordrecht, 1995), p. 93.
¹⁶*Physics of Group IV Elements and III-V Compounds*, edited by O. Madelung, M. Schulz, and H. Weiss, Landolt-Börnstein New Series, Group III, Vol. 17, Pt. a (Springer, Berlin, 1982).
¹⁷G. Arnaud, J. Allegre, P. Lefebvre, H. Mathieu, L. K. Howard, and D. J. Dunstan, Phys. Rev. B **46**, 15 290 (1992).
¹⁸D. Gershoni, J. M. Vandenberg, S. N. G. Chu, H. Temkin, T. Tanbun-Ek, and R. A. Logan, Phys. Rev. B **40**, 10 017 (1989).
¹⁹G. Ji, D. Huang, U. K. Reddy, T. S. Henderson, R. Houdre, and H. Morkov, J. Appl. Phys. **62**, 3366 (1987).
²⁰D. Gershoni, J. S. Weiner, S. N. G. Chu, G. A. Baraff, J. M. Vandenberg, L. N. Pfeiffer, K. West, R. A. Logan, and T. Tanbun-Ek, Phys. Rev. Lett. **65**, 1631 (1990); K. Kash, D. D. Mahoney, and H. M. Cox, *ibid.* **66**, 1374 (1991); D. Gershoni, J. S. Weiner, S. N. G. Chu, G. A. Baraff, J. M. Vandenberg, L. N. Pfeiffer, K. West, R. A. Logan, and T. Tanbun-Ek, *ibid.* **66**, 1375 (1991).
²¹S. Pescetelli, A. Di Carlo, and P. Lugli, Phys. Rev. B **56**, R1668 (1997).
²²G. Goldoni, F. Rossi, E. Molinari, and A. Fasolino, Phys. Rev. B **55**, 7110 (1997).
²³W. Langbein, H. Gislason, and J. M. Hvam, Phys. Rev. B **54**, 14 595 (1996).
²⁴G. W. Bryant, P. S. Julienne, and Y. B. Band, Superlattices Microstruct. **20**, 601 (1996).
²⁵E. Kapon, D. M. Hwang, and R. Bhat, Phys. Rev. Lett. **63**, 430 (1989).
²⁶W. Wegscheider, L. N. Pfeiffer, K. W. West, and R. E. Leibenguth, Appl. Phys. Lett. **65**, 2510 (1994).